Distinct insulating state below the Curie point in $Pr_{0.7}Ba_{0.3}MnO_3$

A. K. Heilman,[1] Y. Y. Xue,[1] B. Lorenz,[1] B. J. Campbell,[2] J. Cmaidalka,[1] R. L. Meng,[1] Y. S. Wang,[1] and C. W. Chu[1,*]
[1]*Texas Center for Superconductivity, University of Houston, Houston, Texas 77204-5932*
[2]*Materials Science Division, Argonne National Laboratory, Argonne, Illinois 60439*
(Received 5 November 2001; revised manuscript received 6 March 2002; published 5 June 2002)

Magnetization, resistivity, thermal expansion, thermopower, and neutron powder diffraction data are presented for the perovskite manganite $Pr_{0.7}Ba_{0.3}MnO_3$. A distinct ferromagnetic insulating state, similar to that observed in the $La_{0.88}Sr_{0.12}MnO_3$ system, is observed in the temperature range between the paramagnetic-ferromagnetic transition at $T_{FM} \approx 180$ K and the broad metal-insulator transition near $T_p = 120$ K. The large *A*-site cation-size mismatch appears to suppress the ferromagnetic double-exchange interactions relative to the competing ferromagnetic superexchange interactions, thereby giving rise to the ferromagnetic insulating state.

DOI: 10.1103/PhysRevB.65.214423 PACS number(s): 75.30.Vn, 75.30.Et

I. INTRODUCTION

The physics responsible for the colossal magnetoresistance (CMR) in the manganites of the form $A_{1-x}A'_xMnO_3$ (with A = trivalent rare-earth cation and A' = divalent cation) is still a topic of debate in spite of the recent intense research activity.[1] In the framework of the widely accepted double-exchange (DE) mechanism with the Jahn-Teller (JT) distortion,[2,3] the resistivity is dominated by the carrier-hopping rate between the adjacent Mn sites. Thus, the decrease in scattering due to the ordering of the $Mn^{+3/+4}$ spins below the ferromagnetic (FM) transition temperature, T_{FM}, causes a drop in ρ. In particular, T_{FM} should be coincident with the peak temperature of the resistivity T_p if the sample is an insulator above T_{FM}. This has been confirmed in manganites with small *A*-site cation mismatch,[4] $\sigma^2 = \Sigma_i\ y_i r_i^2 - \langle r_A \rangle^2$ (where y_i is the concentration, r_i is the ionic radius of the *A*-site ions, and $\langle r_A \rangle$ is the mean ionic radius).[1] However, in manganites with large σ^2, it has been reported that T_p systematically drops below T_{FM} with increasing σ^2 over a broad range of σ^2.[4–9] The presence of minor impurity phases/grain boundaries,[4,9] a carrier-localization due to disorder,[5,10] and mesoscopic chemical inhomogeneities (e.g., conducting La-Ca-Mn-O with embedded insulating Gd-Ca-Mn-O)[7] have all been invoked to explain this separation of T_p and T_{FM}. Some manganites with large $\langle r_A \rangle$ and σ^2 have also been reported to exhibit a spin-glass insulating (SGI) state at low temperatures.[6] To explore these issues surrounding the large σ^2 manganites, high-quality ceramic samples of $Pr_{0.7}Ba_{0.3}MnO_3$ (PBMO) were synthesized, which possess a strong lattice disorder ($\sigma^2 \approx 0.0178$ Å^2, $\langle r_A \rangle = 1.266$ Å) due to the large size difference between the Pr^{+3} and the Ba^{+2} ions. No secondary phases were detected by x-ray diffraction or energy dispersive x-ray.

Several key results are presented in this work. (1) There exists a 60 K temperature difference between T_{FM} (≈ 180 K) and T_p (≈ 120 K). (2) There are distinct anomalies in the thermal expansion coefficient (α) both at T_{FM} and near T_p. (3) The thermoelectric power (S) and resistivity (ρ) both indicate activated carrier-transport above T_p and metalliclike transport below T_p. The activation energy between T_{FM} and T_p is rather different from those observed above T_{FM}. (4) An anomalous drop in the low-field field-cooled magnetization (M_{FC}) occurs with cooling across T_p. (5) A large magnetoresistance (MR) is observed over a wide temperature range that extends below both T_{FM} and T_p. All these are rather different from those observed in a $Pr_{0.7}Sr_{0.3}MnO_3$ (PSMO) sample with a smaller $\sigma^2 \approx 0.0036$ Å^2 ($\langle r_A \rangle = 1.218$ Å). (6) Neutron diffraction data of PBMO reveal a broad structural phase transition near T_p in addition to the PM-to-FM transition at T_{FM}. These data can be interpreted as evidence of two distinct FM states below T_{FM} in the PBMO sample: a ferromagnetic-metallic state (FMM) and a ferromagnetic-insulating state (FMI), similar to those recently observed in $La_{0.88}Sr_{0.12}MnO_3$,[11] which are proposed to be the result of competition between the DE and super-exchange (SE) interactions.

II. EXPERIMENT

Ceramic samples of Pr-Ba(Sr)-Mn-O were prepared by solid-state reaction of powders of Pr_6O_{11}, $SrCO_3$, $BaCO_3$, and MnO_2 with the stoichiometric compositions. These were ground and die pressed into pellets before preliminary reactions in air at 900–1000 °C for 16 h. The samples were then reground and heated at 1100 °C, 1200 °C, and 1250 °C for 16 h in air and finally slow cooled to room temperature.

The composition of the PBMO sample was analyzed using a JEOL JXA 8600 electron microprobe. A stoichiometry Pr:Ba:Mn:O = 0.69:0.302:1:3.04 with a spread of ±2% for the cations and ±5% for the oxygen was observed over the whole surface of the sample. These measurements allow us to conclude that the sample is homogeneous to the length scale of 1 μm. The PSMO sample exhibits a comparable degree of homogeneity. Measurements of M_{FC} and ρ were made simultaneously inside a quantum design superconducting quantum interference device magnetometer, S was measured using an apparatus previously described in detail in Ref. 12, and α was measured using the strain-gage technique. The value of ρ was measured by the standard four-lead technique, employing a model LR-400 bridge by Linear Research, Inc. Time-of-flight neutron powder diffraction (NPD) measurements were conducted from 10 K to 300 K on the SEPD instrument at the Argonne National Laboratory Intense Pulsed Neutron Source. Rietveld structure refinements employed the GSAS software suite.[13]

 ©2002 The American Physical Society

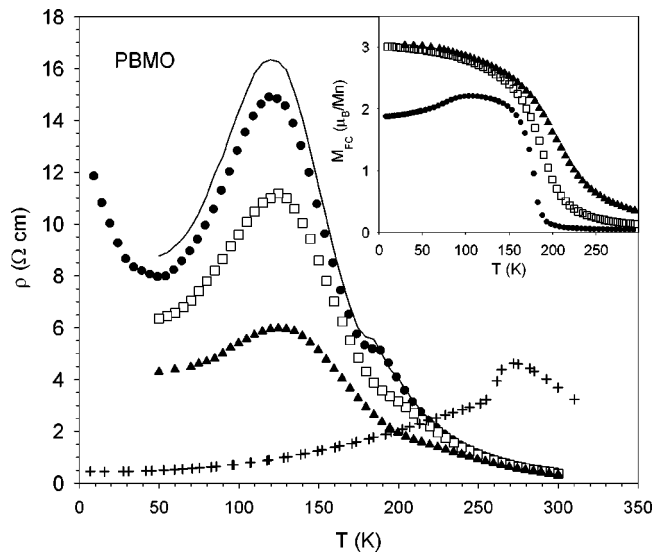

FIG. 1. Resistivity vs temperature in different fields. Solid line: PBMO, $H=0$; ●: PBMO, $H=0.1$ T; □ : PBMO, $H=1$ T; ▲: PBMO, 3 T; + : PSMO, $H=0$. The inset shows the field-cooled magnetization of PBMO at $H=0.1$, 1, and 3 T, respectively.

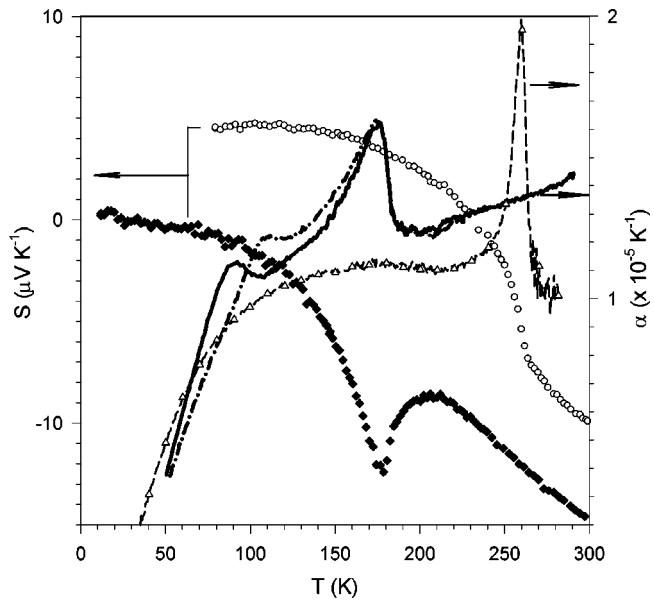

FIG. 2. The thermoelectric power of PBMO (♦) and PSMO (○) (left axis). The thermal expansion coefficient of PBMO (solid line for cooling and dash-dotted line for warming) and PSMO (Δ with dash line) are shown using the right axis. All data are in zero applied field.

III. RESULTS AND DISCUSSION

The M_{FC} data in applied magnetic fields of 0.1, 1.0, and 3.0 T are shown in the inset of Fig. 1. The temperature inflection point is taken as the PM-to-FM transition temperature ($T_{FM}\approx 180$ K at 0.1 T). The corresponding field-dependent ρ is shown in Fig. 1, where the peak resistivity at a zero applied field occurs at a temperature $T_p\approx 120$ K, which is well below T_{FM}. At zero applied field, ρ shows activated transport behavior, $\rho\propto\exp[\Delta/T]$ both above T_{FM} and between T_p and T_{FM}.[1] There is, however, a noticeable anomaly in ρ near T_{FM}, which appears to be smeared out with increasing field.

A significant MR is observed over a large temperature range extending well below T_p, in contrast to typical CMR systems in which the MR is strongly peaked at T_{FM}, and negligible deep in the ferromagnetic-metallic region.[1] The spins of PBMO, however, are well-aligned below T_{FM}, as indicated by the quick saturation of M with cooling at $H\geqslant 1$ T in Fig. 1. In fact, the M_{FC} at 1 T reaches 2.5 μ_B/Mn at 150 K, comparable with both the value (≈ 3 μ_B/Mn) observed at 10 K and the saturation moment (≈ 3.7 μ_B/Mn) expected for typical manganites at this doping level. No significant MR, therfore, would be expected around the much lower temperature $T_p\approx 0.65T_{FM}$ based on the DE models. In addition, there are no recognizable ρ versus M correlations, which would be characteristic of spin scattering.[14] The decrease of ρ with H at 50 K, for example, is almost the same either from 0 to 1 T or from 1 to 3 T, although the corresponding increases of M differ by more than tenfold (Fig. 1). All these suggest that factors other than the average spin alignment also play a role. It should be pointed out that the observed onset of the FM moment at T_{FM}, the quick saturation of M with both cooling and magnetic field, the temperature dependence of ρ, and the strong MR between T_{FM} and T_p, are also inconsistent with an SGI state, such as that reported in Ref. 6.

The separation of T_p and T_{FM} has been previously observed in several different high σ^2 manganites, for example, $Nd_{0.7}Ba_{0.3}MnO_3$,[5] $Th_{0.35}(Ba_xSr_yCa_z)MnO_3$,[6] and $(La_{1-x}Gd_x)_{0.7}Ca_{0.3}MnO_3$.[7] The large size-mismatch in these compounds makes chemical phase separations, i.e., insulating grain boundaries and/or mixed phases, a strong possibility. Therefore S, which is regarded as a volume-average measurement and is insensitive to both grain boundaries and minor impurities, has been determined in zero field and is shown in Fig. 2. The $|S|$ of low σ^2 manganites, such as PSMO, near the optimal doping level is usually large (10 μV/K or larger) and insulatorlike with a $1/T$ dependence above T_{FM}, but drops immediately across the transition before reaches a plateau of a few μV/K at lower T. The S of PBMO does follow the rule above T_{FM}, indicative of activated polaron transport.[15] It, however, jumps to an even negative value with cooling across T_{FM}, indicating that the sample is still in a bulk insulating state (likely also dominated by polaron transport) between T_{FM} and T_p with an even larger activation energy. The distinguishable insulatorlike S, both above and immediately below T_{FM}, confirms that the bulk of PBMO is still in an insulating state somewhere below T_{FM}. The expected transition to a metallike S is rather broad and does not finish until well below T_p, a fact attributed to a phase separation between T_{FM} and T_p, as demonstrated in the NPD data below.

Above T_p, the NPD data yield a crystal structure with *Ibmm* symmetry as reported by Jirak *et al.* for high-temperature $Pr_{0.65}Ba_{0.35}MnO_3$,[16] which has been equivalently described in the *Imma* setting for a number of other $A_{0.7}A'_{0.3}MnO_3$ systems.[17,18] The *Ibmm* setting should be assumed throughout the present work unless otherwise noted.

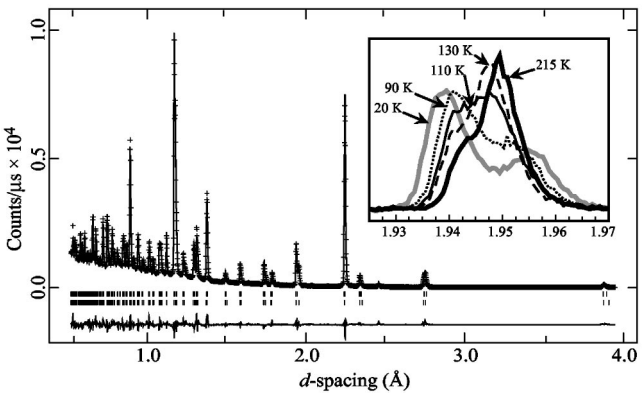

FIG. 3. Neutron powder diffraction data from PBMO at 10 K. Both the data and the difference curve from the Rietveld refinement of the two-phase model are shown. The top and bottom rows of markers indicate *Ibmm* and *I*4/*mcm* peak positions, respectively. The inset contains the temperature dependence of the (220, 004) peak pair.

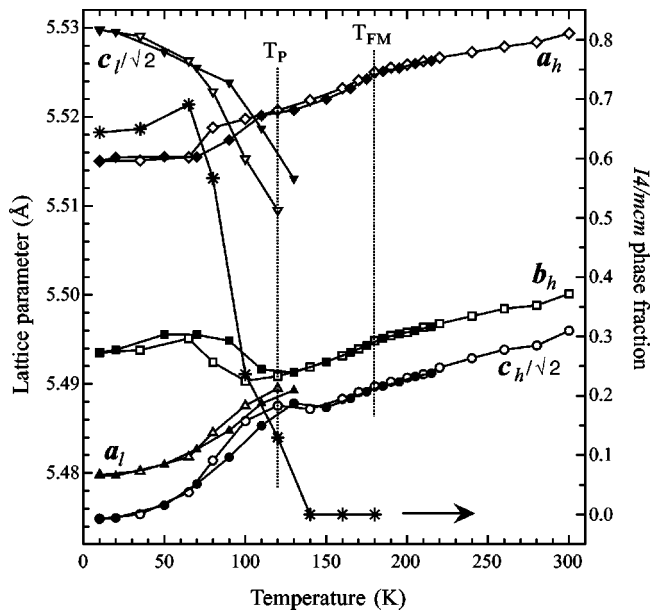

FIG. 4. The lattice parameters of the high-temperature ("*h*") *Ibmm* and low-temperature ("*l*") *I*4/*mcm* phases of PBMO from 10 K to 300 K. Open and filled symbols indicate data collected during warming and cooling, respectively. The phase fraction of the *I*4/*mcm* phase of PBMO is indicated by asterisks (*).

While somewhat unusual, the relation $b<a$ observed here indicates a Mn-O-Mn bond angle that varies slightly from 180°.[18] After correcting this relation, which was difficult to resolve in earlier NPD data,[19] one finds our room-temperature $Pr_{0.7}Ba_{0.3}MnO_3$ lattice parameters [$a=5.5294(1)$ Å, $b=5.5001(1)$ Å, $c=7.7725(1)$ Å] to be nearly identical to those of Ref. 16. Near T_p, the NPD data reveal a phase transition to a low-temperature structure with *I*4/*mcm* symmetry, which only goes to 75% completion down to the lowest temperatures measured (10 K), producing a mixed-phase region over all the temperature range explored below T_p. This structural transition is also hysteretic, occuring primarily between 90 K and 130 K on warming and between 70 K and 110 K on cooling. The results of the Rietveld refinement at 10 K are shown in Fig. 3 and the temperature-dependent lattice-parameters appear in Fig. 4. The (220/004) peak pair is shown as a function of temperature in the inset of Fig. 3, where the smaller (004) peak moves from the left- to the right-hand side of the plot due to the reversal of c and $(a+b)/2$ in the low-temperature *I*4/*mcm* phase. The lattice parameters of the *Ibmm* phase display a rather weak peak at T_{FM}. The refined FM moment rises to 3.7 μ_B/Mn between T_{FM} and T_p, as expected, and lies along the c axis of the structure. In the mixed-phase region, however, the resolution of the data was insufficient to properly treat the FM moments of the two phases separately, so that the moments were constrained to be equal and directed along the c axis. No significant JT distortions were observed in the *Ibmm* or *I*4/*mcm* structures, which differ primarily in their octahedral-tilt patterns.[16] This may be closely associated with the good size match between (Pr, Ba) and Mn.

The ceramic thermal-expansion coefficient measurements in Fig. 2 corroborate the NPD observations, where α exhibits a well-defined nonhysteretic peak near T_{FM}, which is attributed to the ferromagnetic transition, as well as a broad hysteretic peak in the vicinity of T_p, (i.e., ≈ 91 K on cooling and ≈ 107 K on warming). The fact that the hysteretic peak at T_p, which is associated with much larger lattice parameter changes, is smaller than the peak at T_{FM}, reflects a gradual change of the phase fractions in the mixed-phase region. This interpretation is in agreement with the S observed, which shows an extremely broad transition from the insulatorlike one somewhere below T_{FM} to the metallike one below 80 K (Fig. 2). It should be noted that the noticeable anomaly of α as well as the appearance of a new phase in NPD around T_p suggest that the ρ peak may be associated with a change in the bulk property instead of grain boundaries. To verify, the temperature-dependent ceramic-sample striction (L/L_0) is plotted in Fig. 5 for both PBMO and PSMO samples. The L/L_0 of PBMO, including a distinct kink at T_{FM} and only smaller broad bumps near T_p (although they can be noticed clearly in the $\alpha = d \ln L/dT$ of Fig. 2) agrees nicely with the phase-weighted unit-cell volume determined from the NPD data, and that of PSMO exhibits only one kink at T_{FM}. While L/L_0 is nearly identical for these two materials in the "mostly *I*4/*mcm*" region of PBMO below 80 K, the transformation around T_p in PBMO is accompanied by a significant volume increase, when viewed in comparison to that of PSMO in the FMM state. Above the ferromagnetic transition temperatures, the two curves are nearly coincident once again. The transition around T_p seems to be associated with a phase transition related the change of the cell volume.

The widely separated values of T_{FM} and T_p are unusual compared to most low-σ^2 manganites, such as PSMO, which undergoes a simultaneous PM-to-FM and metal-insulator transition at $T_{FM} \approx 263$ K (Figs. 1 and 5). The well correlations among the NPD, S, L/L_0, and ρ data here, however, suggests that the *Ibmm* phase of PBMO might be FMI above T_p. The natural of this intermediate FMI state in PBMO can be better understood by comparing the cell volumes of

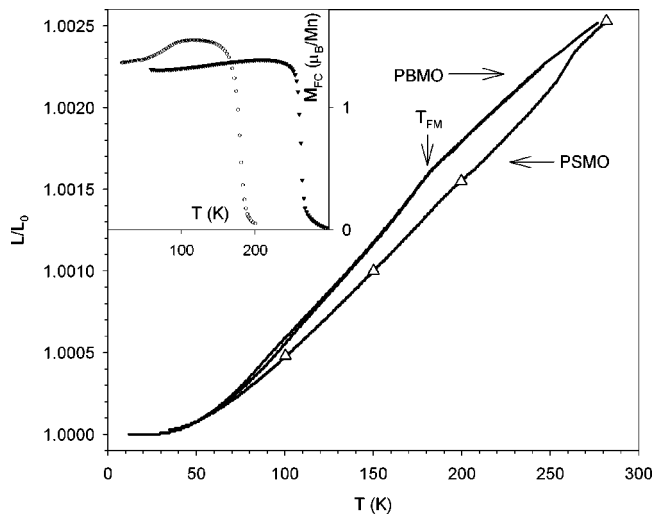

FIG. 5. Ceramic-sample striction (L/L_0) vs temperature for the PBMO and PSMO samples in zero field. Hysteresis can be noticed between 70 to 150 K for PBMO (top one associated with cooling). Inset: The field-cooled magnetization in a field of 500 G for the PBMO sample (open symbols) and the PSMO sample (filled symbols).

PBMO and PSMO (Figs. 4 and 5). The insulating *Ibmm* PBMO cells above T_p appear to be larger than that expected from the FMM cells of PSMO. It has been proposed and later confirmed that the cell volume of manganites is mainly determined by the nature of the Mn-O bonds.[21] In particular, the bonds associated with SE interactions are typically longer than those of DE interactions. Such an increase of cell volumes at the FMM-FMI transition has been previously reported in $La_{0.88}Sr_{0.12}MnO_3$ and $La_{0.875}Sr_{0.125}MnO_3$,[11,20] where it was attributed to the difference in the relative strengths of the DE and SE interactions; the FMM state being dominated by DE interactions and the FMI state being dominated by competing SE interactions. We, therefore, tentatively attribute the intermediate FMI state in PBMO to similar competitions between SE and DE. The local lattice distortions in high-σ^2 manganites significantly suppress the DE interaction through their lower carrier mobility, which shows up as both the 80 K suppression of T_{FM} and the tenfold increase of the resistivity above T_M from PSMO to PBMO (Fig. 1). The contributions of SE, hence, may become dominated in an intermediate temperature range until the increase of the carrier mobility with further cooling which allows the DE to dominate again. In such a scenario, the phase separation observed over a broad T range will also be rather natural based on the possible mesoscale inhomogeneity of the lattice distortion.

Terashita *et al.* recently explained the FMI state in the $(La_{1-x}Gd_x)_{0.7}Ca_{0.3}MnO_3$ system in terms of Gd- and La-rich clusters with distinct electronic and magnetic properties.[7] The Gd-rich regions would still be in the insulating PM state between T_{FM} and T_p, and break the percolating paths. In such a scenario, $|S|$ should decrease through T_{FM}, and M_{FC} increase through T_p (as additional parts of the sample enter the FM state) on cooling. Because the opposite behavior is observed in the present study of PBMO, the FMI state of PBMO appears to be more consistent with the SE-dominated FMI state of $La_{0.875}Sr_{0.125}MnO_3$. The cell volumes in the two cases is certainly consistent with the interpretation.

The M_{FC} of the PBMO and PSMO in a low field of 500 G is compared in the inset of Fig. 5. For the PSMO sample, the M_{FC} in the FMM state plateaus below T_{FM} and remains virtually constant as the temperature decreases. For the PBMO sample, the M_{FC} also plateaus just below T_{FM}. Below 100 K, however, the M_{FC} starts to decrease toward a significantly lower plateau. The difference in M_{FC} between the two plateaus is almost 10%. It diminishes with the increase of H and disappears above 1.0 T (Fig. 1). The trend is again consistent with the M_{FC} observed in $La_{0.875}Sr_{0.125}MnO_3$.

IV. CONCLUSION

A distinguishable FMI state exists in $Pr_{0.7}Ba_{0.3}MnO_3$ between $T_{FM} \approx 180$ K and $T_p \approx 120$ K. The structural changes at the ferromagnetic transition are minor, whereas the ferromagnetic-insulating phase with *Ibmm* symmetry transforms incompletely to a low-temperature ferromagnetic metal with *I*4/*mcm* symmetry over a broad range of temperatures below T_p. Magnetization, resistance, and thermopower measurements suggest that the FMI state of $Pr_{0.7}Ba_{0.3}MnO_3$ is similar to the FMI state of $La_{1-x}Sr_xMnO_3$ ($0.1 \leqslant x \leqslant 0.14$), which occurs due to an unusual dominance of ferromagnetic superexchange interactions. An enhanced tendency toward electron localization due to lattice disorder in cation-size-mismatched perovskites may weaken the influence of the DE interaction, and offers a natural interpretation of the FMI state. Comparisons with $Pr_{0.7}Sr_{0.3}MnO_3$, which has a small *A*-site cation-size mismatch and no intermediate FMI state, support these conclusions.

ACKNOWLEDGMENTS

The authors thank D. K. Ross for electron microprobe measurements, J. Kulik for TEM data, and Simine Short for assistance with NPD data collection. This work is supported in part by NSF Grant, the T. L. L. Temple Foundation, the John and Rebecca Moores Endowment, and the State of Texas through TCSUH, and at LBNL by DOE. Research at ANL was supported by the U.S. Department of Energy, Office of Science under Contract No. W-31-109-ENG-38.

*Also at Lawrence Berkeley National Laboratory, 1 Cyclotron Road, Berkeley, CA 94720 and Hong Kong University of Science and Technology, Hong Kong.

[1] See A.P. Ramirez, J. Phys.: Condens. Matter **9**, 8171 (1997) for a review.

[2] C. Zener, Phys. Rev. **81**, 440 (1951); *ibid.* **82**, 403 (1951).

[3] A.J. Millis, P.B. Littlewood, and B.I. Shraiman, Phys. Rev. Lett. **74**, 5144 (1995); A.J. Millis, Phys. Rev. B **53**, 8434 (1996).

[4] Lide M. Rodriguez-Martinez and J. Paul Attfield, Phys. Rev. B **54**, 15 622 (1996).

[5] J.M.D. Coey, M. Viret, L. Ranno, and K. Ounadjela, Phys. Rev. Lett. **75**, 3910 (1995).

[6] A. Maignan, C. Martin, G. Van Tendeloo, M. Hervieu, and B. Raveau, Phys. Rev. B **60**, 15 214 (1999).
[7] H. Terashita and J.J. Neumeier, Phys. Rev. B **63**, 174436 (2001).
[8] L.M. Rodriguez-Martinez, H. Ehrenberg, and J.P. Attfield, J. Solid State Chem. **148**, 20 (1999).
[9] L.M. Rodriguez-Martinez and J.P. Attfield, Phys. Rev. B **63**, 024424 (2000).
[10] L.Sheng.D.Y. Xing, D.N. Sheng, and C.S. Ting, Phys. Rev. Lett. **79**, 1710 (1997).
[11] H. Nojiri, K. Kaneko, M. Motokawa, K. Hirota, Y. Endoh, and K. Takahashi, Phys. Rev. B **60**, 4142 (1999).
[12] Y. Song, unpublished; A.K. Heilman, Y.Y. Xue, Y.Y. Sun, R.L. Meng, Y.S. Wang, B. Lorenz, C.W. Chu, J.P. Franck, and Weimin. Chen, Phys. Rev. B **61**, 8950 (2000).
[13] A. Larson and R. B. von Dreele, *GSAS Manual*, Los Alamos Report No. LAUR-86-748, Los Alamos National Laboratory, 1986.
[14] M.F. Hundley, M. Hawley, R.H. Heffner, Q.X. Jia, J.J. Neumeier, J. Tesmer, J.D. Thompson, and X.D. Wu, Appl. Phys. Lett. **67**, 860 (1995); J.Z. Sun, L. Krusin-Elbaum, S.S.P. Parkin, and G. Xiao, *ibid.* **67**, 2726 (1995); B. Chen, C. Uher, D.T. Morelli, J.V. Mantese, A.M. Mance, and A.L. Micheli, Phys. Rev. B **53**, 5094 (1996).
[15] P. M. Chaikin, in *Organic Superconductivity*, edited by V. Z. Kresin and W. A. Little (Plenum, New York, 1990), p. 101–115.
[16] Z. Jirak, E. Pollert, A.F. Andersen, J.C. Grenier, and P. Hagenmuller, Eur. J. Solid State Inorg. Chem. **27**, 421 (1990).
[17] P.G. Radaelli, M. Marezio, H.Y. Huang, and S.W. Cheong, J. Solid State Chem. **122**, 444 (1996).
[18] F. Damay, Z. Jirak, M. Hervieu, A. Maignan, B. Raveau, G. Andre, and F. Bouree, J. Magn. Magn. Mater. **190**, 221 (1998); Z. Jirak, F. Damay, M. Hervieu, C. Martin, B. Raveau, G. Andre, and F. Bouree, Phys. Rev. B **61**, 1181 (2000).
[19] Z. Jirak, private communication.
[20] B. Martínez, R. Senis, Ll. Balcells, V. Laukhin, J. Fontcuberta, L. Pinsard, and A. Revcolevschi, Phys. Rev. B **61**, 8643 (2000).
[21] J.B. Goodenough, Phys. Rev. **100**, 564 (1955).